STScI | SPACE TELESCOPE SCIENCE INSTITUTE

Instrument Science Report WFC3 2023-01

WFC3/UVIS Post-flash: Stability of the LED and Creation of Time-Dependent Reference Files

C. Martlin, J. Green

March 6, 2023

Abstract

An LED provides WFC3/UVIS with the capability to increase background levels with user-directed flashes that can help to improve charge transfer efficiency (CTE) in images with low backgrounds. Analyzing data from 2012-2021, we completed several tests to check for changes in power and illumination pattern of the LED onto the UVIS detector over time. ***By studying the subarray and full-frame post-flashed dark images over time we find there is a decrease in the measured post-flash mean over time. This change is in line with previously observed changes in WFC3 sensitivity for filters with similar spectral properties as the LED, measured to be about ∼ 0.2% per year (Calamida et al. 2021, Marinelli et al. 2022).*** *We interpret this to indicate that there is no systematic decay in the LED illumination that cannot be attributed to previously reported detector sensitivity changes. Following that result, we investigated whether there was any time dependence in the post-flash reference files if binned by yearly or biyearly cadences. We used these newly created time-dependent reference files to produce FLC images for various GO science data and determined that the*

time-dependent post-flash reference files do improve the quality of the science data without significantly affecting the measured noise. We report that the average mean measurement of our science images change up to 2.64% with the time-dependent reference files while the standard deviation change is measured to be less than 1/1000 of a percent. We determined that using yearly reference files was the most accurate calibration available as it balances the number of input files, which affects the signal-to-noise, and the time covered by the input data, which affects the change in measured post-flash. ***We therefore delivered new yearly post-flash reference files to the WFC3/UVIS data calibration pipeline*** `calwf3`***.*** *They have been available as of December 2022 and data requested from MAST since their delivery is post-flash corrected with the new reference files.*

---

1 Introduction

Post-flashing is an instrument capability used to increase the background in WFC3/UVIS images via the onboard LED. This is necessary because UVIS exposures with low backgrounds, such as large field observations, experience poor CTE leading to sources smearing their counts during readout (WFC3 Instrument Hand Book, section 6.9). The reference files generated by the post-flash calibration program provide the removal of this flash to yield accurate counts for science images. The post-flash is applied to an entire exposure, and is therefore present in both the background and the source pixels. For proper calibration, the post-flash needs to be accurately subtracted from the image image along with dark current and bias.

In Section 2, we explain some in-depth information related to the set up and functioning of the post-flash LED to provide users a background necessary to understand later portions of this study.

In Section 3, we describe the data used in our study.

In Section 4, we look for changes in the brightness and behavior of the LED by investigating the normalized mean value of post-flashed darks over time. We also compare our analysis to recently published results that quantify a change in WFC3/UVIS sensitivity over time (Calamida et al. 2021, Marinelli et al. 2022).

In Section 5, we describe how we tested newly generated time-dependent reference files that were averaged over a variety of cadences and compare them to the current, or sometimes referred to in this report as "original", reference file which was an average of all post-flash data between 2012 - 2016. We then match the test time-dependent reference files to example General Observer (GO) data taken within the same year(s) as the corresponding reference file to produce updated FLC files. We then analyze these newly calibrated FLCs to investigate the effects of including time dependence in creating the post-flash reference file. Finally, we determine the optimal recommended cadence by checking differences between the cadences and their effect on the average measurements and noise on the science data.

In Section 6, we describe, in-depth, the creation of the new time-dependent yearly post-flash reference files to prepare them for delivery.

In Section 7, we include a description of the test of the post-flash LED count rate and include a table of the newly measured count rates and for each flash current.

In Section 8, we list our conclusions.

In Appendix A, we provide a table of the previous flash duration and current for each flash level prior to the 2020 update and after the 2020 update. These values are incorporated in the Astronomer's Proposal Tool (APT) and users do not access them directly, instead only needing to request the flash level desired (in e-/pixel).

In Appendix B, we provide information on the newly delivered time-dependent postflash reference files.

2 Background Post-flash Information

The LED on WFC3/UVIS provides users with the ability to add diffuse illumination onto the CCD following an observation, and to customize the added level. Using options available in APT, an observer request the LED to illuminate the array to a specific level (in increments of 1 e-/pix) to add additional diffuse background just prior to readout in order to increase CTE (Anderson et al. 2021). The LED adds a diffuse background by illuminating one of two shutters - shutter A or shutter B. This added background is then removed by the `calwf3` data calibration pipeline, which uses a shutter-dependent reference file. It is critical that the programmed post-flash duration achieves the user-requested background level as this ensures the image is corrected appropriately by the pipeline.

Of note is that the LED used for post-flashing is placed in between the shutter and the UVIS detector within the WFC3 instrument configuration. This means that the UVIS filter wheel, which is located before the shutter apparatus, is inaccessible to the LED and does not affect the flash applied to the detector. A dark image is a calibration observation taken with the shutter closed to measure the inherent noise/charge within the detector at that time and is therefore, also, not affected by choice of filter. Anything measured on a calibrated post-flashed dark image is a measurement of the LED output bouncing off the internal side of the shutter and onto the UVIS detector.

Lastly, the LED used to provide the source of the post-flash on the detector has three current settings - low, medium, and high; only the former two are used operationally. This setting controls how bright the LED is which, in turn, affects the count rate measured by the detector. The count rate of the two currents was originally measured in Biretta et al. (2013) and is reported in Section 7. That count rate was used to calculate the needed flash duration to apply an expected flash level to the UVIS detector. In this study we have reported a change in the count rate of the low and medium settings as measured in 2020. This change has already been accounted for by updates in the table used by APT to calculate

the flash duration for a specific flash level as requested by a user. A couple of flash levels had their flash current changed from low to medium current, which means those levels also have a decrease in the overhead time needed. These updates are further discussed in Section 7.

3 Data

This study uses three main data sets. In detail, they are:

1. Subarray dark images taken at various flash levels with low current to be used to verify the stability of the LED;
2. A series of full-frame medium current dark images which have a high signal-to-noise and are ultimately used to create the post-flash reference file;
3. Individual science images with few or no bright sources to test the efficacy of the new reference files.

The first two are products of long-term calibration proposals and the third type is gathered from public science data available through the MAST archive.

3.1 Post-flash Monitor and Calibration Data

The first two data categories were observed as calibration programs over the course of each HST cycle between 2012 and 2022, averaging 84 full-frame images and 216 subarray images per cycle. The individual programs from each cycle are listed in Table 1. For each program, the observational cadence and the image properties for subarray and full-frame observations are similar; details can be found in the Phase II proposal files available online and linked to in Table 1. Lastly, all data, both subarray and fullframe, were reduced using the current `calwf3` (3.6.2) which applied calibrations such as CTE correction, and gain adjustment to convert from e-/DN to e-/pixel.

3.2 Reference File Testing Data

For each year of post-flash data we proceeded to select a single UVIS science image from various GO programs in order to test the effect of our new post-flash reference files on low background data, which would be most affected by a change in the post-flash reference file. For consistency, each dataset we decided on met the following criteria:

1. No bright/saturated sources were present in the FOV;
2. No other known image anomalies - dragon's breath, satellite trail, filter ghost, etc. (Gosmeyer et al. 2017) - were present in the images;

Cycle	Years	Proposal ID
Cycle 20	2012-2013	13078
Cycle 21	2013-2014	13560
Cycle 22	2014-2015	14006
Cycle 23	2015-2016	14372
Cycle 24	2016-2017	14535
Cycle 25	2017-2018	14984
Cycle 26	2018-2019	15573
Cycle 27	2019-2020	15718
Cycle 28	2020-2021	16398
Cycle 29	2021-2022	16570

Table 1: Calibration programs to test the LED stability and create post-flash reference files.

3. No large, diffuse nebulosity was apparent;

4. Each image was taken in the same filter (F336W), which helps mitigate any possible filter-dependent differences.

The selected images are listed in Table 2.

Year	Cycle	Proposal ID	Rootname	Association ID
2012	Cycle 19	12527	ibru01knq	IBRU01040
2013	Cycle 20	12959	ic1707bmq	IC1707020
2014	Cycle 21	13297	icau22uqq	ICAU22020
2015	Cycle 22	13804	icmx05qlq	ICMX05030
2016	Cycle 23	14164	icw806qtq	ICW806050
2017	Cycle 24	14610	idb616edq	IDB616030
2018	Cycle 25	15275	idn011e6s	IDN011030
2019	Cycle 25	15083	idle02ayq	IDLE02010
2020	Cycle 25	15275	idn073crq	IDN073030
2021	Cycle 27	15857	ie0o61lyq	IE0O61LYQ

Table 2: Science observations used to test updates to the post-flash reference file. We have included the rootname of the individual test files as well as their association ID to aid in locating them in MAST. All images have a flash level set to values between 8 to 12 (e-/second).

4 LED Stability and UVIS Detector Sensitivity

4.1 Tracking the Normalized Mean Post-flash Value Over Time

Tracking the stability of the LED output over time is important to monitor the health of the system and to ensure that the post-flash reference files are up-to-date with current detector illumination.

Subarray image comparison. Following the same procedure as Martlin et al. (2017), in this study we normalized the mean electrons in every UVIS2 C1K1C subarray image to: (1) the mean electrons of the first 2012 observation in order to track the changes in brightness over time and (2) to the duration of the individual image in order to allow comparison across the APT updates in 2020. The overall brightness, i.e. mean electrons of the subarray, has decreased by $\sim 0.18\% \pm 0.01\%$ per year in both shutter A and B settings (Figure 1). These changes are equivalent, within the uncertainty, to the photometric sensitivity changes of the WFC3/UVIS detector (Calamida et al. 2021, Marinelli et al. 2022) measured for external data taken through the F775W and F814W filters.

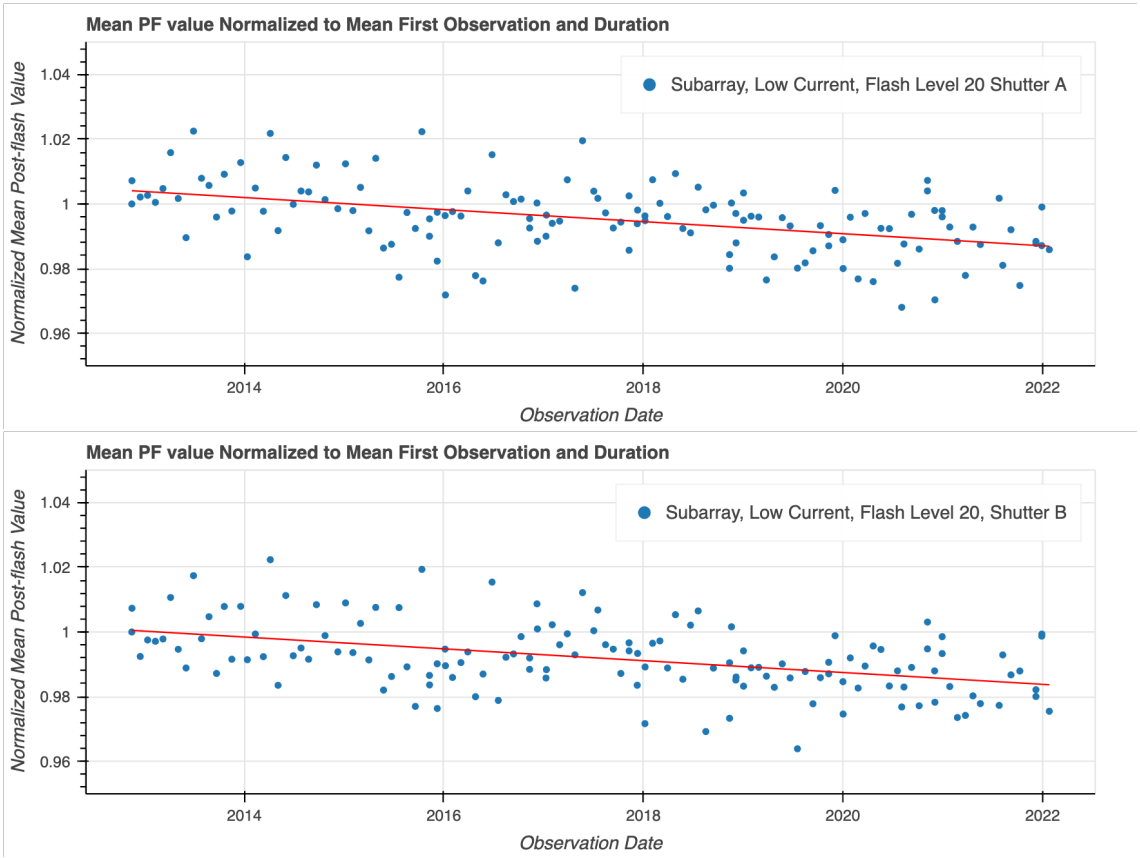

Figure 1: Measurement of the individual mean electrons of all subarray observations between 2012-2022 that were post-flashed at a level of 20 e-, normalized to the first 2012 observation mean electrons and normalized by their flash duration. Observations were post-flashed using shutter A (top) or shutter b (bottom). This subarray is located in the bottom left of quadrant C of UVIS2. The linear fits (red line) on each plot indicate a decrease of $0.19\% \pm 0.03\%$ per year for shutter A and $0.18\% \pm 0.03\%$ per year for shutter B, consistent with the sensitivity changes of UVIS external data taken in filters with bandpasses encompassing the spectral output of the LED lamp (Calamida et al. 2021, Marinelli et al. 2022).

Those two filters were chosen because they encompass the spectrum of the LED; figure 2 shows the spectral output of the LED (from Kurtz et al. 2017). The LED output peaks at $\sim$ 8100 Å and covers the range of just above 7400 Å to just below 8900 Å. There is no

WFC3/UVIS filter that matches this range perfectly, but there is a sufficient overlap of this range between the two filters F775W and F814W. We have included the throughout plots of both filters in Figure 3 (WFC3 Instrument Handbook, Dressel, L., 2019). Filter F775W's transmission ranges from just under 7000 to 8600 Å, while filter F814W's transmission ranges from 7000 to $\sim$ 9800 Å.

As the decrease of the measured LED output over time is within the two sigma level of the decrease in measurements over time of external data taken at similar wavelengths this suggests that the **sensitivity of the detector, and not changes in the LED output itself, is causing this decrease**.

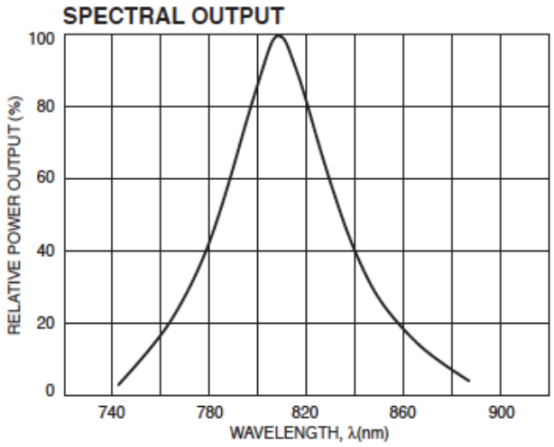

Figure 2: Throughput for the LED used to post-flash UVIS data.

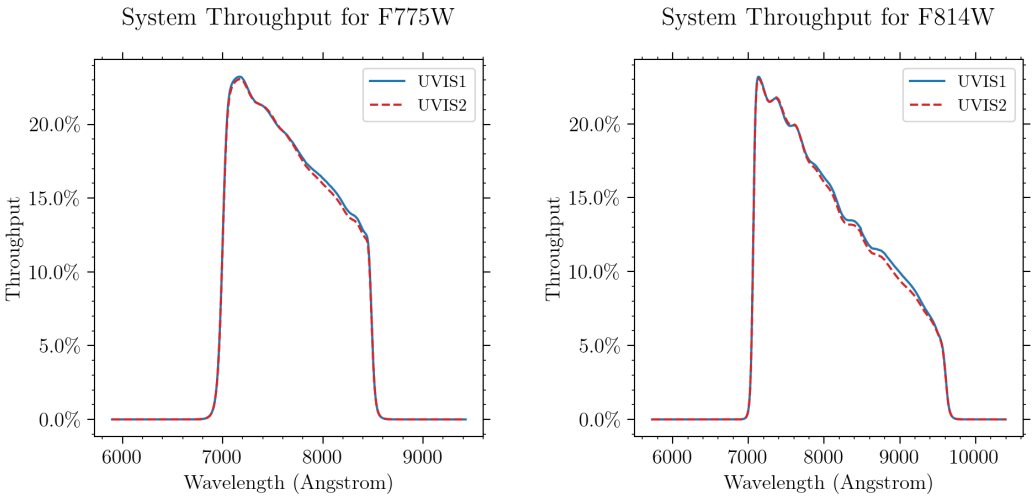

Figure 3: Integrated system throughputs for the two filters with bandpasses encompassing the LED spectral output for F775W and F814W.

Full-frame image comparison. In addition to the subarray check, we also assess the

normalized mean electrons for all full-frame dark images over time to ensure the changes seen in the subarray were consistent with the changes for the entire detector. The full-frame images are comprised of both UVIS1 and UVIS2, while the subarray is the lower left portion of the bottom left quadrant C of UVIS2.

As seen in Figure 4 and recorded in Table 3 the LED output averaged over the full-frames decreases by 0.20% ± 0.01% per year for shutter A and 0.21% ± 0.01% per year for shutter B. Again, we find these changes to be consistent with the measured changes reported for external UVIS images as well, within uncertainty, which indicates this decrease is not due to the LED and that the LED output continues to be stable over time.

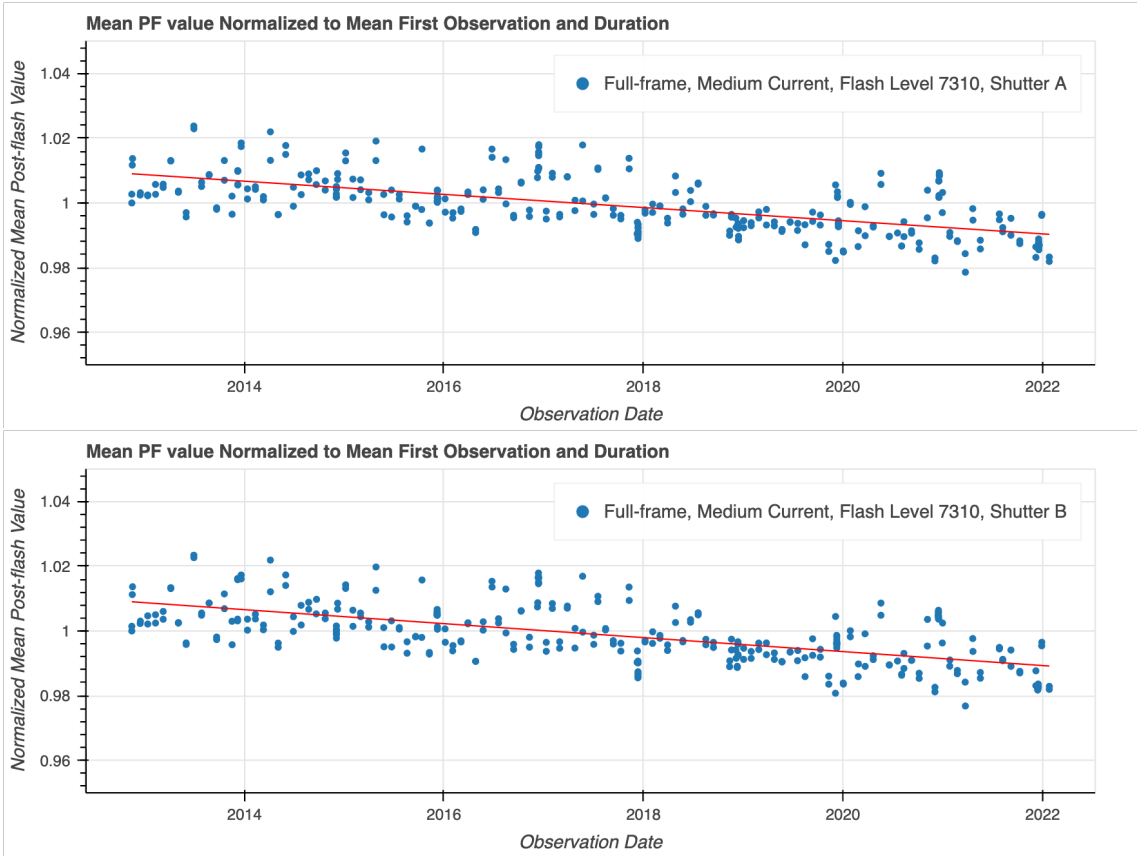

Figure 4: Measurement of the individual mean electrons of all full-frame dark observations between 2012-2022 that were post-flashed at a level of 7310 e-, normalized to the first 2012 observation mean electrons and normalized by their flash duration. Images were post-flashed with shutter A (top) and shutter B (bottom). The linear fit (red line) for Shutter A indicates a decrease of 0.20% ± 0.01% per year and for shutter B measures a 0.21% ± 0.01% decrease per year, consistent with the sensitivity changes of UVIS external data taken in filters with bandpasses encompassing the spectral output of the LED lamp (Calamida et al. 2021, Marinelli et al. 2022).

UVIS Aperture	Post-flash Shutter and Flash Level	Number of Images	slope ± error (%/year)
Subarray (UVIS2)	A, 20e-	139	-0.19 ± 0.03
	B, 20e-	139	-0.18 ± 0.03
Full-frame (UVIS1, UVIS2)	A, 20e-	314	-0.20 ± 0.01
	B, 20e-	314	-0.21 ± 0.01

Table 3: Measured change in LED output.

5 Reference File Updates: Testing Time Dependence

5.1 Creating Time Dependent Reference Files

Following previous post-flash generation methods (Biretta et al. 2013, Kurtz et al. 2017), we used varying sets of full-frame, 0.5-second darks that are post-flashed for 100 seconds with the medium current, or about 7500 e-/pix. In previous studies, post-flash reference files were then created from a *median value of all data covering all available years* for each shutter A and B. Here we evaluated reference files created from *median values over various cadences*. We ultimately find that using a time-dependent post-flash reference file improves the accuracy of the pipeline subtraction of the post-flash.

This is supported by the noticeable shift in the overall values of individual reference file pixels which decreases in counts over time. Figure 5 visualizes this shift well by plotting a histogram of the electrons/second of a newly created yearly reference file for 2021 versus the electrons/second for the original pipeline reference file (which is the median of all data from 2012 - 2016). The electrons/second in the 2021 reference file are very similarly distributed to the original reference file, implying the illumination shape onto the detector has not changed drastically, but overall the electrons measured by the pixels shifted to lower values; we investigate this further in Section 5.2. We have also included the 2017 reference file to illustrate that this shift is a gradual one over time and differences between data prior to 2017 would be difficult to statistically detect. Over time, the overall shift of the post-flash measurement by the detector has caused differences up to 0.2 e-/s from the original reference file, as seen at the peak in the 2021 histogram versus the original reference file histogram in Figure 5.

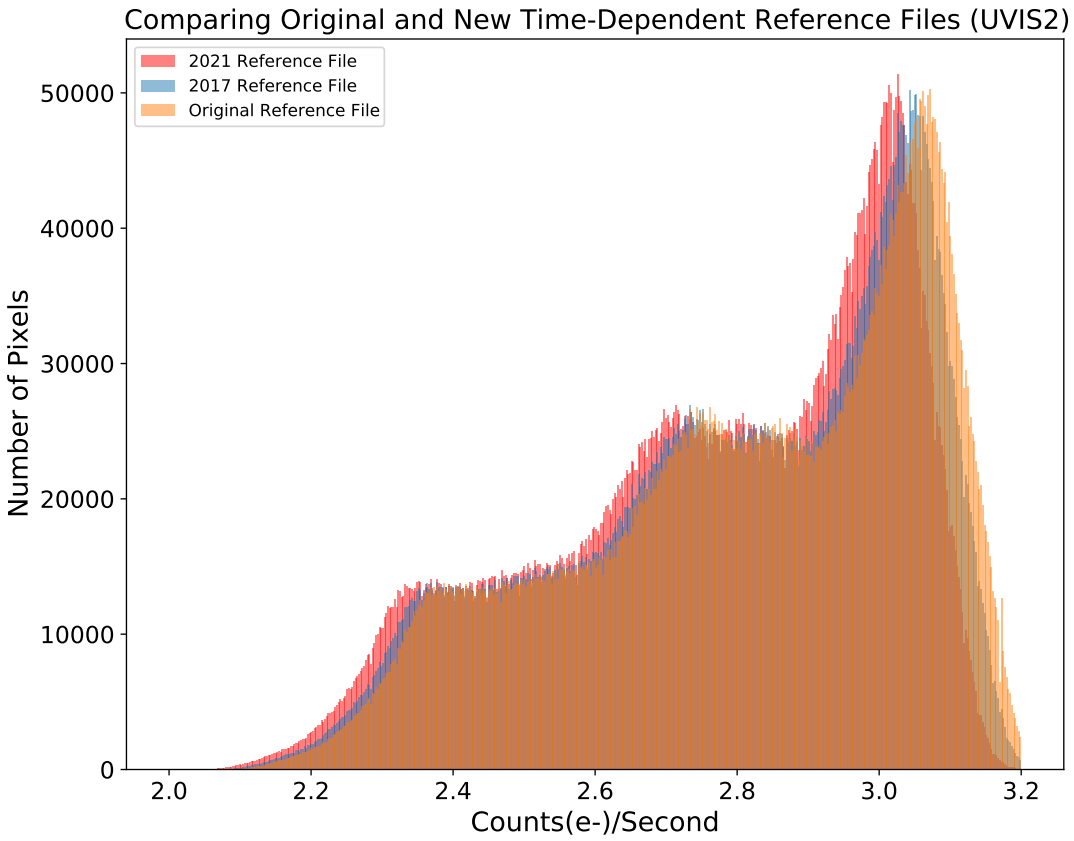

Figure 5: Comparison of electrons/second for pixels within UVIS2 between the 2021 time-dependent reference file (red), the 2017 time-dependent reference file (blue), and the original time-independent reference file (orange). The gradual leftward shift of the electrons/second of the 2017 and 2021 reference files demonstrates the need of a time-dependent reference file.

5.2 Comparing New Reference Files to Original

Computational Inspection. An investigation into the yearly reference files efficacy was based on the ratio of each yearly reference file to the original pipeline reference file generated from files taken from 2012-2016. In Table 4 we see, not unexpectedly, that each individual year differs slightly overall when a ratio is created between that year's reference file and the original pipeline reference file. That change is also larger in value the further from 2016 the reference file gets, which is also further from data included in the creation of the original reference file.

We have included these mean measurements of the ratio for the entire UVIS detector (full-frame) and for Quadrant C. Kurtz et. al (2017) reported that Quadrant C has the largest variation in the post-flash illumination across its area when compared to all other UVIS quadrants. As that area has the largest post-flash variations across it, we posited that the largest ratio measurements would be there as well. We do find that the standard deviation tends to be larger for that area, versus the full-frame, but that the Quadrant C mean of the ratio of the yearly reference file to the original reference file is consistent with the full-frame measurements. The tabulated values help illustrate the importance of switching from a single post-flash reference file over all time to individual reference files for each year as it shows an increasing overall change in the measured value of the post-flash over time.

	Full-Frame	**Quadrant C**
Year	Mean	Mean
2012	1.0009 ± 0.0032	1.0009 ± 0.0043
2013	1.0017 ± 0.0031	1.0017 ± 0.0041
2014	1.0006 ± 0.0029	1.0007 ± 0.0035
2015	0.9977 ± 0.0029	0.9978 ± 0.0036
2016	1.0002 ± 0.0039	1.0005 ± 0.0058
2017	0.9940 ± 0.0051	0.9943 ± 0.0084
2018	0.9917 ± 0.0068	0.9921 ± 0.0124
2019	0.9895 ± 0.0113	0.9899 ± 0.0218
2020	0.9911 ± 0.0156	0.9916 ± 0.0307
2021	0.9849 ± 0.0172	0.9855 ± 0.0338

Table 4: The mean and standard deviation of the ratio of each yearly reference file to the original post-flash reference file. We have included these stats for the entire reference file in columns 2 and 3 and the stats for just quadrant C in columns 3 and 4.

Visual Inspection. We also completed a visual inspection of all reference file ratio images to help us distinguish whether there was a change in the spatial distribution of the full-frame illumination over time. If the ratio of the old reference file to the new yearly reference file had spatial structure it could indicate that the spatial distribution of the LED illumination may be changing over time. Considering the average mean of each ratio of the reference images, measured in Table 4, is on the order of 1% or less, we were not expecting any large structural changes in the reference files. After the visual inspection and several unsuccessful attempts to apply contours (as done in Kurtz et al. 2017) to the ratio images, we conclude

that there are no noticeable changes in the spatial distribution of the illumination of the LED over time.

5.3 Comparing Yearly and Biyearly Testing Cadence

We followed the study of the yearly reference files to the original reference file with a final comparison of the biyearly and yearly reference files to determine the appropriateness of using the yearly version going forward. In Figure 6, we compare the electrons per second for all UVIS2 pixels of the 2020-2021 biyearly reference file to the electrons per second for all UVIS2 pixels of the 2021 yearly reference file. There is no significant difference in the overall shape of the histograms and only a very small shift in the values of the reference files. We can see the level of this difference by comparing the mean and standard deviation of each, which we have listed in Table 5. The mean differs by less than 0.005 e-/sec while both have a standard deviation of 0.567 e-/sec. Therefore, we conclude there is no statistically significant effect from binning the reference files over two years compared with one year. This leads us to using a yearly reference file to best correct for the ongoing changes in the UVIS detector sensitivity. As of December 8th 2022, `calwf3` will now select a reference file from the same year as the science dataset when correcting for applied post-flash.

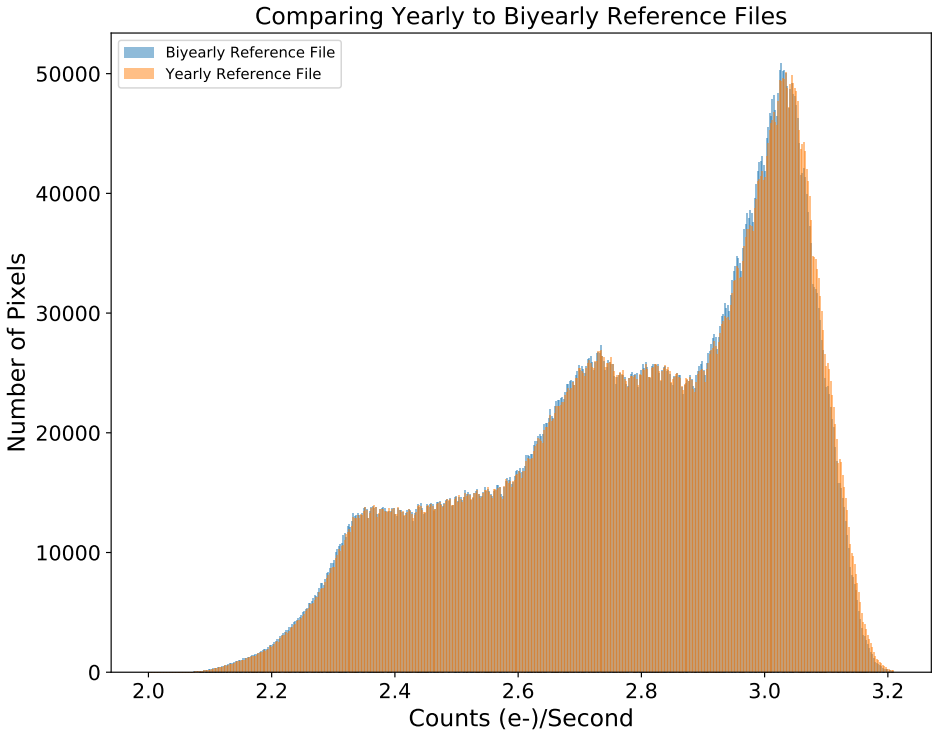

Figure 6: Comparison of electrons/second for pixels within UVIS2 of the biyearly reference file (blue) vs. electrons/second for pixels within UVIS2 of the yearly reference file (orange).

Cadence: Year of Reference File	Mean (e-/sec)	Standard Dev. (e-/sec)
Yearly: 2021	2.694	0.567
Biyearly: 2021/2020	2.689	0.567

Table 5: Table of the mean and standard deviation of the 2021 yearly post-flash reference file and the 2021/2020 biyearly post-flash reference file. We see the mean is different by about 0.005 e-/sec and their standard deviations match.

5.4 Testing with Science Data

As previously stated, the calibration pipeline, prior to December 2022, has been using a single post-flash reference file which is created from a median of post-flashed darks taken from 2012 to 2016. We proposed this would be sub-optimal as reference files created from data taken closest in time to the science data would more accurately capture the concurrent state of the detector. However, combining multiple years of datasets improves uncertainties in reference files, which was more important at the beginning of post-flashing as the time range and information available about the full effects of the post-flash on science data was still growing. In order to compare the effect of a time-dependent reference file on science data noise we used the yearly reference files to calibrate science data from 2012 - 2021.

First, we measured the relative error budgets of example science data, as calibrated by MAST with the original time-independent post-flash reference file. To measure the relative error budgets we began with the images listed in Table 2, and randomly selected five sample 200×200 square pixel regions scattered in different areas of the UVIS2 chip. We then computed the overall statistics of those regions (such as mean, median, standard deviation, etc). We compared those statistics with the same datasets processed with post-flash reference files created from varying cadences of data (1, 2 and 5 year splits). To increase the readability of this report, we have included this data only for the measurements of the science data calibrated with the original time-independent reference file and the science data calibrated with the yearly cadence of time-dependent reference files. In Table 6, the average standard deviation and average mean value in electrons of all 5 regions for each example science image from 2012 to 2021, when corrected with the original post-flash reference file, is listed. Further, we have provided the difference from that original average mean and original average standard deviation of the same regions corrected, instead, with the yearly post-flash reference file.

While we are working with small numbers, due to the regions being chosen specifically to contain mostly diffuse background measurements, we do see an increasing change in the average mean of the regions over time when correcting with a time-dependent post-flash reference file versus the original time-independent post-flash reference file. The mean difference of the time-dependent reference file averages to about 0.01% in 2012 up to a difference of 2.64% in 2021. This gradual increase in the value of the average mean difference is attributed to the growing difference between the original post-flash reference file (made from 2012-2016 data) and the new yearly post-flash reference files. Further, the difference in the standard deviations we measure over time is minimal, for example 0.00014 e-/sec for the 2021 data compared to 0.00019 e-/sec for 2012. All of the average mean standard deviations listed in Table 6 measure to less than 1/1000 percent of the original standard deviation

measurement with the time-independent reference file This illustrates that the change to using fewer input images to create yearly reference files, instead of using many over several years, does not significantly impact the noise of science image measurements.

Year	Rootname	Mean (e-/sec)	Standard Dev. (e-/sec)	Mean Difference (e-/sec)	Standard Dev. Difference (e-/sec)
2012	ibru01knq	21.4	223.5	0.024	0.00019
2013	ic1707bmq	16.5	170.5	0.015	0.00009
2014	icau22uqq	31.4	248.9	0.034	0.00003
2015	icmx05qlq	14.5	179.3	0.068	0.00019
2016	icw806qtq	9.5	142.3	0.039	0.00014
2017	idb616edq	15.9	268.6	0.11	0.00002
2018	idn011e6s	15.2	175.5	0.081	0.00023
2019	idle02ayq	15.0	192.4	0.137	0.000004
2020	idn073crq	7.5	100.1	0.124	0.00015
2021	ie0o61lyq	10.1	189.6	0.270	0.00014

Table 6: Table of the average standard deviation and average mean of all 5 regions, picked to contain few sources and mostly diffuse background, for each test science image when corrected with the original post-flash reference file, in columns 2 and 3. And in columns 4 and 5, the difference in the average standard deviation and average mean measurements of all 5 test regions for each test science image when corrected with the new yearly reference file.

6 Reference File Updates: Creation and Delivery

As a result of the testing in Section 5 we determined that time dependence was worth implementing and found that a yearly cadence is a small enough time span to account for changes in the detector without causing a significant change in the noise of typical low background science images.

The improvement from yearly reference files has only became significantly large enough to distinguish over a longer timeline. We can see this change over ten years within Figure 4. We find that the mean value decreases by 0.203 +/- 0.014% per year for Shutter A full-frame observations, and 0.215 +/- 0.015% per year for Shutter B, showing that Shutter A and B measurements are consistent within uncertainty. The mean value decrease is in line with the change in detector sensitivity measured from external data sources (Calamida et al., 2021; Marinelli et al., 2022).

In creating the low current, un-binned, yearly reference files and the medium current, un-binned, yearly reference files we followed the same process as Biretta et al. (2013) and Kurtz et al. (2017), but we have adjusted the input post-flash images by separating them into separate years. The only exception is the 2012 reference file; as the post-flash capability was

enabled in November 2012 with Cycle 20, we include data from November 2012 to November 2013 in order to allow for a full year of data.

The process to create the post-flash reference files is as follows: all images were calibrated with `calwf3` version 3.6.2 to correct for CTE, bias level, dark correction, cosmic rays, etc. Following calibration we stacked the images by year into a single median combined image while masking any bad pixels. As all input images being used to create the reference files are high signal-to-noise post-flashed darks, we scale them by dividing by the exposure time followed by multiplying by the previously found scale factor 0.03639 (Biretta et al. 2013) to create the finished reference file product: a 1-second, low current median stack that is dependent on shutter and year. Following previous practice, we then scaled all 20 low current reference files by 28.96 to then create the medium current, 1-second post-flash reference files for each shutter and year from 2012 - 2021 (Biretta et al. 2013). Information about the number of individual reference files that went into creating each yearly reference file can be seen in the table in Appendix B.

7 Updates to Post-flash Count Rate

In the previous study Biretta et al. (2013), there was non-linearity noted in the relationship between the LED flash duration and the recorded electrons per second per pixel (e-/sec/pixel). This non-linearity was seen to differ between the low current and the medium current flashes as a function of time and is recorded in Table 7.

Flash duration	Low current	Medium current
< 3 sec	2.62 e-/sec/pixel	73 e-/sec/pixel
> 3 sec	2.44 e-/sec/pixel	67 e-/sec/pixel

Table 7: Count rate used to compute flash durations in 2013.

Therefore, at the start of this study, we began by investigating the measured count rate vs. flash duration for the newest data available. Since the change in the count rate is largest in the most recent data, we only include data from the first 7 months of 2020 in Figure 7, which was the most recent data to when we were investigating. To illustrate the change from the first recorded check of the count rate we also include the same data used in Biretta et al. (2013) which was from November 15th, 2012. We note that there was a change in the count rate as measured by the detector over time, as shown by the majority of the 2020 count rates being lower on Figure 7 than the 2012 values, regardless of flash duration.

To ensure users get the requested background values applied to their images, we have provided updated durations for all flash levels available in APT, from 3 e-/pix to 25 e-/pix, and changed the flash current for levels 14, 15, 21, 22 e-/pix, see Table 8. The updates to the current level lead to a change in the duration needed to reach the requested flash level because medium current setting provides significantly more output, in e-/sec/pixel, than the low current (Table 7 above as well as the table in Appendix A). These updates were tested and installed in APT in July 2020. We anticipate that with the continuing degradation of

CTE and as the overall sensitivity of the WFC3 detector continues to change, users will likely require higher post-flash levels in future years to ensure images with low background reach the recommended level of 20 e-/pix or above, so we also provided new flash durations to APT to allow observers to request flash levels 26 e-/pix to 40 e-/pix.

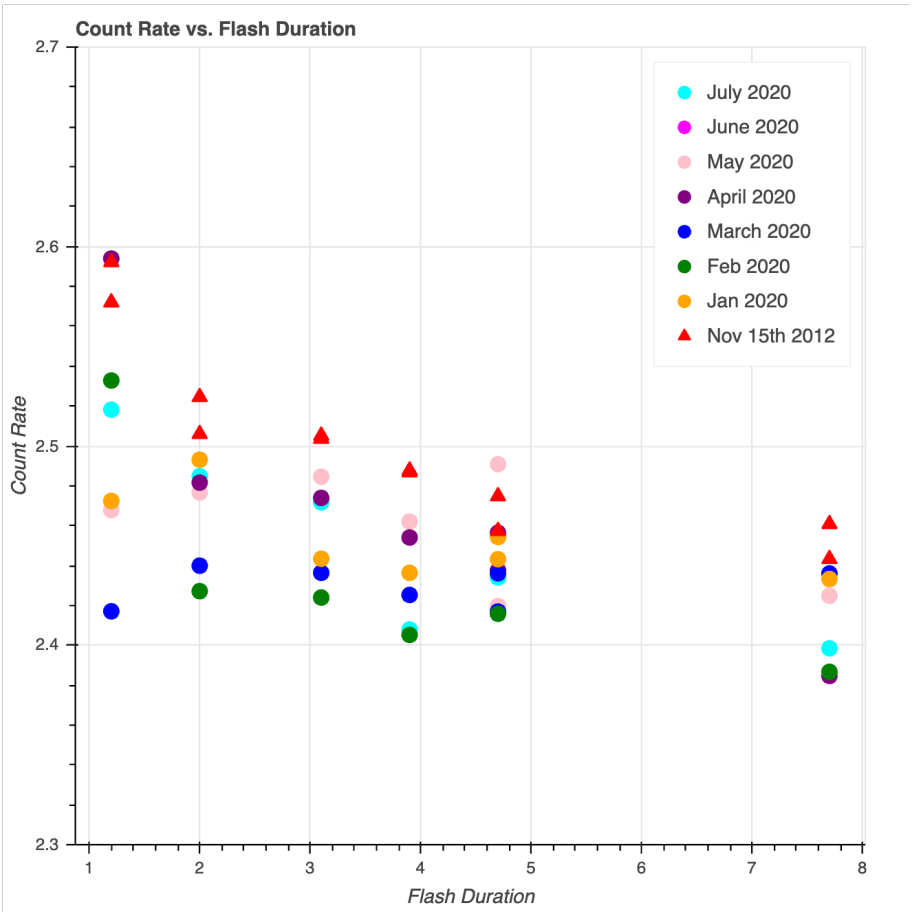

Figure 7: Flash duration (sec) vs. measured count rate (e-/sec/pixel) for dark current calibration datasets taken in 2020, prior to APT changes. The red triangles are the 2012 data and the circles are results from 2020.

Flash duration	Low current	Medium current
< 3 sec	2.5 e-/sec	70.5 e-/sec
> 3 sec	2.4 e-/sec	69.5 e-/sec

Table 8: Count rate used to compute updated APT flash durations in 2020.

Users should note that these updates in APT are built into the system itself so no special actions need to be taken besides ensuring their version of APT is up to date when creating proposals. A full table of all updates to flash durations and flash currents is available in Appendix A, which also lists the previous values for reference.

8 Conclusion

We have investigated the long-term stability of the WFC3 LED. Analyzing data from 2012 to 2022, we performed several tests of the LED to check for changes in the output and illumination over time and found a decease in the normalized mean value of the post-flash applied to a dark image over time, for both subarray and full-frame images. Further, we compared this decrease in the post-flash output to the decrease in the photometric measurements of external data and found them effectively the same. Given the post-flash data are internal, i.e. the LED light is bounced off the closed shutter blade down onto the detector, and the photometric data analysed and presented in other UVIS reports are external, i.e. the light beam travels the entire optical HST+instrument path, we conclude the change in the measured post-flash over time is not a change in the LED output itself but is likely due to the sensitivity of the UVIS detector. We also investigated the spatial distribution of the full-frame illumination by the LED and did not find any significant changes.

Lastly, we investigated the effect of using time-dependent post-flash reference files instead of a single monolithic reference file by generating a series of test post-flash reference files averaged over data from various time cadences. We used these newly created time-dependent reference files to produce FLC images for various calibration and GO science data and determined that the time-dependent post-flash reference files do improve the quality of the FLC data without noticeably increasing the noise of the science images. While there is currently no noticeable effect from binning the reference files over two years compared with one year, as the sensitivity of the UVIS detector continues to change over time we have decided to use a yearly cadence for reference files to allow more precise calibration of the changes to the post-flash over time. As of December 2022, the new yearly post-flash reference files (listed in Appendix B) are in the MAST automated calibration pipeline and all post-flashed UVIS data have been reprocessed.

Acknowledgments

The authors thank Aidan Pidgeon for additional testing of the reference files prior to delivery. We also thank Sylvia Baggett for numerous discussions and guidance on this work. We thank the referees Mariarosa Marinelli, Amanda Pagul, and Benjamin Kuhn for their diligent and helpful reviews.

References

Anderson, J., Baggett, S., & Kuhn, B., 2021. "Updating the WFC3/UVIS CTE Model and Mitigation Strategies", WFC3 Science Report 2021-09.

Biretta, J., & Baggett, S., 2013 "WFC3 Post-Flash Calibration", WFC3 Instrument Science Report 2013-12.

Calamida, A., Mack, J. , Medina, J., Shahanan, C., Bajaj, V., & Deustua, S., 2021. "New time-dependent WFC3 UVIS inverse sensitivities", WFC3 Instrument Science Report 2021-04.

Dressel, L., 2019. "Wide Field Camera 3 Instrument Handbook, Version 11.0" (Baltimore: STScI)

Gosmeyer, C.M., & The Quicklook Team, 2017. "WFC3 Anomalies Flagged by the Quicklook Team". WFC3 Instrument Science Report 2017-22.

Kurtz, H. & Baggett, S., 2017. "Generating the WFC3 UVIS Post-Flash Reference File", WFC3 Instrument Science Report 2017-13.

Martlin, C. & Baggett, S., 2017. "Long-term Stability of the Post-Flash LED Lamp", WFC3 Instrument Science Report 2017-03.

Marinelli, M., Bajaj, V., Calamida, A., Khandrika, H., Mack, J., Pidgeon, A., Shanahan, C. & Som D., 2022. "Monitoring WFC3/UVIS Photometric Sensitivity with Spatial Scans", WFC3 Instrument Science Report 2022-04.

Appendix A - Post-Flash Values Used by APT

	Prior to 2020		**2020 Update**	
APT Requested Flash Level (e-/pix)	Duration (sec)	LED Current	Duration (sec)	LED Current
1	0.4	low	0.4	low
2	0.8	low	0.8	low
3	1.2	low	1.3	low
4	1.6	low	1.7	low
5	2.0	low	2.1	low
6	2.3	low	2.5	low
7	2.7	low	2.9	low
8	3.1	low	3.3	low
9	3.5	low	3.8	low
10	3.9	low	4.2	low
11	4.3	low	4.6	low
12	4.7	low	5	low
13	5.0	low	5.4	low
14	5.4	low	0.2	medium
15	0.2	medium	6.3	low
16	6.2	low	6.7	low
17	6.6	low	7.1	low
18	7.0	low	7.5	low
19	7.3	low	7.9	low
20	7.7	low	8.3	low
21	8.1	low	0.3	medium
22	0.3	medium	9.2	low
23	8.9	low	9.6	low
24	9.3	low	10	low
25	9.7	low	10.4	low
26	–	–	10.8	low
27	–	–	0.4	medium
28	–	–	11.7	low
29	–	–	12.1	low
30	–	–	12.5	low
31	–	–	12.9	low
32	–	–	13.3	low
33	–	–	13.8	low
34	–	–	0.5	medium
35	–	–	14.6	low
36	–	–	15	low
37	–	–	15.4	low
38	–	–	15.8	low
39	–	–	16.3	low
40	–	–	16.7	low

Appendix B - Summary of Delivered Reference Files

Reference File Name	Year	Shutter	Current	Number of Images
6c82015di_fls.fits	2012	A	LOW	28
6c820159i_fls.fits	2012	B	LOW	28
6c820120i_fls.fits	2012	A	MEDIUM	28
6c820154i_fls.fits	2012	B	MEDIUM	28
6c82014ti_fls.fits	2013	A	LOW	32
6c82012mi_fls.fits	2013	B	LOW	32
6c82014li_fls.fits	2013	A	MEDIUM	32
6c820168i_fls.fits	2013	B	MEDIUM	32
6c82016ti_fls.fits	2014	A	LOW	30
6c82013li_fls.fits	2014	B	LOW	30
6c82011ci_fls.fits	2014	A	MEDIUM	30
6c82016ci_fls.fits	2014	B	MEDIUM	30
6c82015li_fls.fits	2015	A	LOW	35
6c82016pi_fls.fits	2015	B	LOW	35
6c82013ti_fls.fits	2015	A	MEDIUM	35
6c82014ci_fls.fits	2015	B	MEDIUM	35
6c82013di_fls.fits	2016	A	LOW	35
6c82013pi_fls.fits	2016	B	LOW	35
6c820163i_fls.fits	2016	A	MEDIUM	35
6c82015hi_fls.fits	2016	B	MEDIUM	35
6c820144i_fls.fits	2017	A	LOW	35
6c82016gi_fls.fits	2017	B	LOW	35
6c82012di_fls.fits	2017	A	MEDIUM	35
6c820128i_fls.fits	2017	B	MEDIUM	35
6c82012hi_fls.fits	2018	A	LOW	35
6c82011gi_fls.fits	2018	B	LOW	35
6c820124i_fls.fits	2018	A	MEDIUM	35
6c82012qi_fls.fits	2018	B	MEDIUM	35
6c82013hi_fls.fits	2019	A	LOW	35
6c82015ti_fls.fits	2019	B	LOW	35
6c82014pi_fls.fits	2019	A	MEDIUM	35
6c820134i_fls.fits	2019	B	MEDIUM	35
6c820139i_fls.fits	2020	A	LOW	38
6c82011li_fls.fits	2020	B	LOW	38
6c82015pi_fls.fits	2020	A	MEDIUM	38
6c82016li_fls.fits	2020	B	MEDIUM	38
6c82011pi_fls.fits	2021	A	LOW	31
6c82014gi_fls.fits	2021	B	LOW	31
6c820130i_fls.fits	2021	A	MEDIUM	31
6c820148i_fls.fits	2021	B	MEDIUM	31